

Light-Scattering Studies on Hydrogen-Bonded Polymer Blends

Dorab E. Bhagwagar, Paul C. Painter, and Michael M. Coleman*

Department of Material Science and Engineering, The Pennsylvania State University, University Park, Pennsylvania 16802-5007

Received May 4, 1994*

ABSTRACT: Phase diagrams for poly(*n*-hexyl methacrylate) blends with a series of styrene-*co*-vinylphenol polymers have been mapped using light-scattering techniques. These are compared to theoretical phase diagrams calculated using an association model that incorporates the various interactions in hydrogen-bonded polymer systems. The thermodynamics of these blends is strongly affected by the competition between the self-associating and interassociating hydrogen bonds and the unfavorable dispersive interactions. The balance of these competing factors controls the temperature and composition of phase separation. The results of the theoretical predictions are found to be in good accord with the experimental phase diagrams. They also help in explaining the molecular weight independence and the skewness (asymmetry) of the phase diagrams.

Introduction

Measurements of the change in scattered intensity between single- and two-phased regions (cloud point determinations) have long been used to delineate phase boundaries in polymer blends. These measurements employ a variety of light-scattering techniques, ranging from the simple visual observation of sample opacity to sophisticated methods employing multichannel analyzers. In this paper, we present phase diagrams obtained by light scattering for some hydrogen-bonded polymer blends.

Motivation for these studies is 2-fold. Over the years we have developed an association model^{1,2} that describes free energy changes upon mixing polymers possessing functional groups capable of strong, specific interactions (such as hydrogen bonds). The model assumes that contributions from the hydrogen-bonding interactions can be separated from the remaining dispersive (nonspecific) interactions. The free energy changes arising from the strong, directionally specific hydrogen bonds are then described in terms of equilibrium constants associated with the bond formation that in many cases can be determined experimentally using infrared spectroscopy. The dispersive interactions, on the other hand, can be modeled by a simple Flory type χ parameter. As this χ parameter accounts for only the purely dispersive interactions, it can be approximated by a solubility parameter approach.³ Miscibility in these systems is then considered a balance between the usually favorable (to mixing) hydrogen bonds and the unfavorable dispersive interactions. The association model has been extensively applied to predict trends in miscibility through "miscibility maps" or "miscibility windows" in a number of hydrogen-bonded polymer systems.¹ Comparison to the complete phase diagram, however, provides a more stringent test for the applicability of the model.

Secondly, it has long been recognized that polymer solutions containing hydrogen-bonding functional groups show unusual phase behavior, including upper critical solution temperature (UCST) and immiscibility loop type phase diagrams.⁴ A number of cloud point experiments⁵ have shown phase separation for polymer blends to be strongly dependent on the strength and number of hydrogen-bonding groups. Recent studies on hydrogen-bonded methacrylic acid copolymer blends have also shown the existence of UCST behavior.⁶ Furthermore, spinodal decomposition studies on blends containing only a small

Table 1. Polymers Employed in This Study

polymers	symbol	M_n	T_g (°C)
poly(styrene- <i>co</i> -vinylphenol) (7 wt % VPh)	STVPh[7]	14 000	108
poly(styrene- <i>co</i> -vinylphenol) (9 wt % VPh)	STVPh[9]	11 000	110
poly(styrene- <i>co</i> -vinylphenol) (50 wt % VPh)	STVPh[50]	42 000	155
poly(<i>n</i> -hexyl methacrylate)	PHMA	55 000	-53
		400 000	-5
poly(<i>n</i> -butyl methacrylate)	PBMA	55 000	21

amount of hydrogen-bonding groups show static and dynamic characteristics very different from "conventional" non-hydrogen-bonded polymer blends.⁷

In this work, we attempt to systematically show the effect of hydrogen bonding on the phase behavior of polymer blends. Random copolymers of styrene and vinylphenol (STVPh) blended with poly(*n*-hexyl methacrylate) (PHMA) are studied. The hydroxyl groups of the vinylphenol and the carbonyl groups of the methacrylate are involved in the hydrogen bonding, with the hydroxyl groups capable of self-associating (by forming hydrogen bonds to themselves) as well as interassociating with the carbonyl groups. The addition of the vinyl phenol in the STVPh influences the hydrogen-bonding capabilities as well as the solubility parameter (and therefore the dispersive interactions) of the copolymer. This complex interplay of all interactions within the system is shown to affect the final phase behavior.

Phase diagrams of styrene-*co*-vinylphenol containing 7, 9, and 50 wt % vinylphenol (denoted as STVPh[7], STVPh[9], and STVPh[50], respectively) with PHMA are mapped by light scattering. Changes in the vinyl phenol content of the copolymer are reflected by alterations in the temperature and position of the phase boundaries. In the Experimental Section, the polymers used, methods of sample preparation, and the light-scattering apparatus are outlined. The following section then describes the results of the experimental work. Our interpretation of these results is deferred to the Discussion. Here we compare the experimental phase diagrams with theoretical predictions from our association model. The association model, which incorporates all the various interactions, is then used as a basis for understanding the observed phase behaviors.

Experimental Section

All the polymers utilized in this study, along with their abbreviations, molecular weights, and glass transition temperatures are summarized in Table 1. The styrene-*co*-vinylphenol

* To whom correspondence should be addressed.

* Abstract published in *Advance ACS Abstracts*, October 15, 1994.

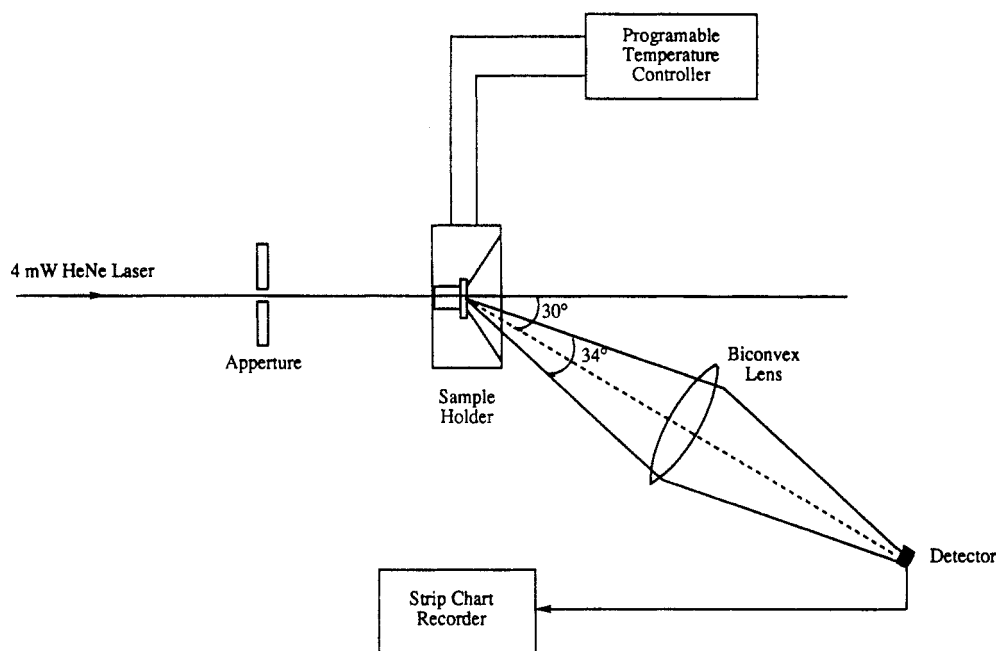


Figure 1. Schematic diagram of the light-scattering equipment.

copolymers with 7 and 9 wt % vinylphenol were synthesized in our laboratory by a procedure described previously.⁸ The poly(*n*-butyl methacrylate) and the lower molecular weight poly(*n*-hexyl methacrylate) were also synthesized in our laboratory by group transfer polymerization.⁹ The higher molecular weight PHMA was purchased from Scientific Polymer Products, Inc., while the styrene-*co*-vinylphenol containing 50% vinylphenol was procured from Hoechst Celanese.

Cloud points were determined using a light-scattering equipment, a schematic representation of which is shown in Figure 1. Light from a 4 mW HeNe laser ($\lambda = 6328 \text{ \AA}$) is incident on the sample, which is housed in a heating cell controlled by an Omega CN-2010 programmable temperature controller. Scattered light is then collected by a biconvex lens, positioned at a 30° angle, and focused onto a laser detector. The laser detector is coupled to a strip-chart recorder which provides information about the intensity of scattering as a function of time (and sample temperature).

Infrared spectra were recorded on a Digilab FTS-60 Fourier transform infrared (FTIR) spectrometer at a resolution of 2 cm^{-1} . Spectra at elevated temperatures were obtained using a SPECAC high-temperature cell mounted in the spectrometer and a Micristar heat controller.

Benzene was used as the common solvent in the preparation of all blends containing STVPh[7] and STVPh[9]. Samples for light-scattering experiments were prepared by codissolving the polymers in requisite compositions to form a 10% (w/v) solution. For each sample, films were cast from these solutions on two thin microscopic glass cover slips. After evaporation of the majority of the solvent, the slides were placed in a vacuum desiccator for a minimum of 48 h and then in a vacuum oven at 80 °C for 24 h. The slides were then carefully sandwiched between a 200 μm copper spacer and annealed for a further hour at 80 °C to form clear, bubble-free samples. For blends containing the STVPh[50] copolymer, methyl isobutyl ketone (MiBK) was the solvent of choice.⁹ Samples were prepared in a similar manner, although heating in the vacuum oven at 110 °C for 24 h and 140 °C for an additional 4 h was necessary for removal of all the solvent. To compensate for the higher boiling point of the solvent thinner samples (50 μm thick) were prepared. Samples for infrared spectroscopy were prepared by solvent casting directly on KBr windows. Drying procedures as described above were then adopted to remove solvent.

Results

The systems that were experimented upon can be divided into two broad categories. Blends employing the

STVPh[7] and STVPh[9] copolymers possess relatively small amounts of hydrogen-bonding groups, while those with the STVPh[50] contained a comparatively larger amount of hydrogen bonding. Phase diagrams (and the method employed in their determination) for these categories were different, necessitating their description in separate sections.

Blends Containing STVPh[7] and STVPh[9]. In the past, infrared spectroscopy has often been used to characterize the degree of association in hydrogen-bonded polymer blends. Although we primarily intend to use light scattering to map the phase diagrams, ease of sample preparation and experimentation make infrared spectroscopy an ideal scouting tool. Formation of hydrogen bonds affects both the carbonyl and hydroxyl stretching frequencies of the infrared spectrum. Qualitative information concerning the degree of molecular mixing for blends containing small amounts of vinylphenol, however, can be readily obtained by studying the hydroxyl stretching region.⁸ Pure STVPh copolymers are characterized by sharp non-hydrogen-bonded (or "free") and broad hydrogen-bonded hydroxyl stretching vibrations at 3525 and approximately 3360–3440 cm^{-1} , respectively. On forming miscible blends with polymers containing carbonyl groups, the "free" hydroxyl peak is effectively suppressed, as most of the hydroxyl groups are now involved in the hydrogen bonding with the carbonyl groups. An example of this is shown in Figure 2A for the STVPh[7]–PBMA blend. Variations in temperature cause small, gradual changes in the ratio of the "free" to hydrogen-bonded hydroxyl groups (a manifestation of the gradual change in the equilibrium constants governing hydrogen-bond formation with temperature), suggesting that these blends are miscible over the temperature range studied. Figure 2B shows the STVPh[7]–PHMA system at a similar blend composition. At lower temperatures, the stretching region is similarly dominated by the hydrogen-bonded hydroxyl band. Above 120 °C, however, the spectra show an abrupt increase in the "free" hydroxyl band. This signifies that around 120 °C the blend has crossed a phase boundary, separating into two phases, one of which is predominantly pure STVPh[7]. Thus, infrared spectroscopy can be used

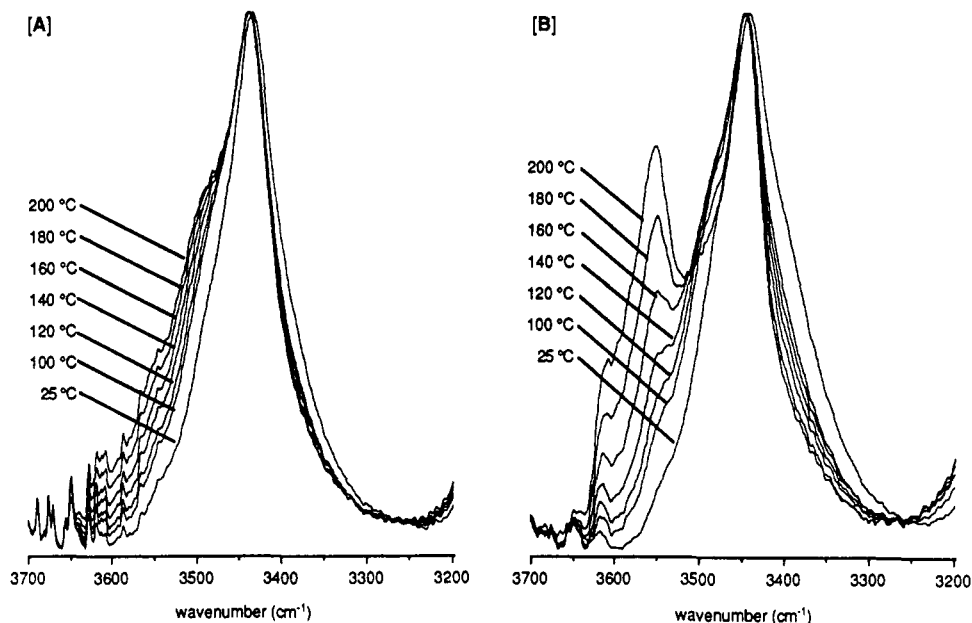


Figure 2. Scale-expanded infrared spectra of the hydroxyl stretching region for [A] the STVPh[7]-PBMA and [B] the STVPh[7]-PHMA blend, at a 40:60 blend composition at the temperatures indicated.

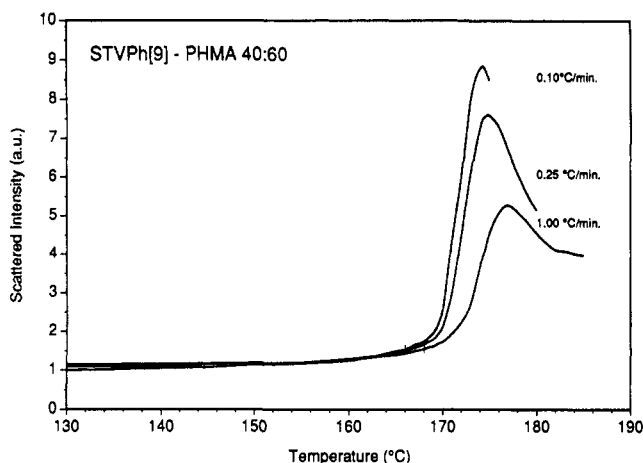


Figure 3. Change in scattered intensity with temperature for the STVPh[9]-PHMA (MW = 55 000) 40:60 blend at different heating rates.

as a quick and efficient method in identifying hydrogen-bonded polymer pairs that phase separate with change in temperature.

More precise information on the temperature of phase separation can be gained from light scattering. Figure 3 shows typical plots of the scattered intensity as a function of temperature at different heating rates. The scattering curves can roughly be divided into three regions. With an initial increase in temperature, the system shows small changes in scattering intensity, probably a result of increase in thermal fluctuations. Then, following the onset of phase separation (shown as small pips in the figure), the scattered intensity undergoes a sharp upturn. For consistency, the onset of phase separation is mathematically taken as the temperature at which the first derivative (slope) of the scattering curve shows a sharp increase. As phase separation proceeds, the scattered intensity continues to rise. Finally the domains formed upon phase separation grow to such a large size that they no longer scatter in the angular range over which the scattering intensity is collected. This shows up as a drop in the scattered intensity after large degrees of phase separation. It is important to emphasize that the observed scattering changes are completely reproducible. The samples can be cooled, annealed for a

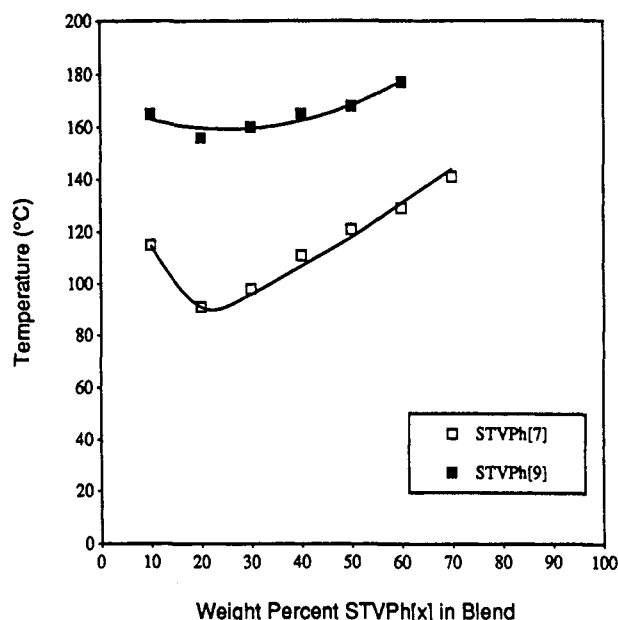


Figure 4. Phase diagrams for the STVPh[7]-PHMA and STVPh[9]-PHMA blends. The solid line is arbitrarily drawn through the phase separation temperatures to aid visual observation. Phase separation temperatures for the STVPh[9]-PHMA blends using PHMA of molecular weights 55 000 and 400 000 are the same within experimental error. Hence the phase diagrams for both the molecular weights are represented by the same curve.

short time (~ 2 h), and then recycled up in temperature to give the same scattering trace within experimental error.

Extrapolating the temperature defining the onset of phase separation at different heating rates to zero heating rate then allows the determination of the "equilibrium" phase separation temperatures (binodals). These are plotted *versus* blend composition as phase diagrams for the STVPh[7]-PHMA and STVPh[9]-PHMA systems in Figure 4. These phase diagrams reveal a couple of interesting features. Firstly, as the amount of hydrogen bonding (or vinylphenol) in the blend increases, the temperature of phase separation exhibits a corresponding increase. This is expected as hydrogen bonding extends the stability (miscibility) of the system, thus increasing

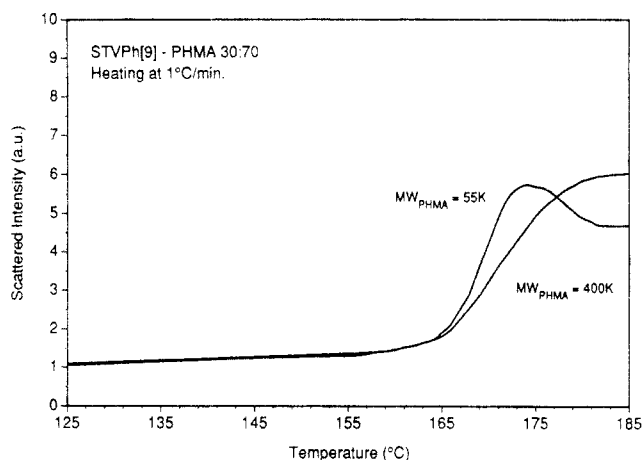


Figure 5. Scattering curve for two STVPh[9]-PHMA blends obtained at a heating rate of 1 °C/min. The molecular weight of the PHMA used in the blends was 55 000 and 400 000.

the temperature at which instability or phase separation commences. Secondly, the diagrams are highly asymmetric, with skewness opposite to that anticipated from a conventional polymer blend.

In order to establish effects of molecular weight on these hydrogen-bonded systems, blends of STVPh[9] with PHMA of differing molecular weight (55 000 and 400 000) were investigated. This system was specifically chosen to minimize the introduction of kinetics effects, as there is about a 100 °C difference between the blend T_g s and phase-separation temperatures. Although there is an order of magnitude disparity in the molecular weights, the phase separation temperatures obtained in both cases were exactly the same (as shown in Figure 4). Comparison of scattering traces at a given heating rate are shown in Figure 5. Although the temperatures at which phase separation start are alike, the curves suggest that the rate at which the separation proceeds is markedly different in the two-cases.

Blends Containing STVPh[50]. Scouting experiments to determine polymers that are miscible with STVPh[50] at room temperature, but phase separate at some elevated temperatures, were again performed using infrared spectroscopy. With the higher concentration of VPh units in these blends, the carbonyl stretching region

is more amenable for qualitative study. Figure 6 shows the “free” and hydrogen-bonded carbonyl bands for blends of STVPh[50] with PBMA and PHMA at similar blend compositions. The initial room temperature spectrum of both blends are comparable to those recorded for completely miscible systems. However, upon heating to 200 °C and cooling back to room temperature, the spectra obtained for the two blends are quite different. As compared to the STVPh[50]-PBMA system, the fraction of hydrogen-bonded carbonyls are not completely recovered for the STVPh[50]-PHMA blend. This implies⁹ the occurrence of phase separation at elevated temperatures for the STVPh[50]-PHMA blend. On cooling to room temperature this two-phase structure is essentially “frozen in”, with a resultant decrease in the degree of hydrogen bonding.

Again, an accurate estimation of the phase-separation temperature can be obtained from light scattering. Due to the higher glass transition temperatures expected in these blends, a reverse quench method, developed by Han and co-workers,⁷ was employed to determine the cloud points. Essentially this method consists of first forming a finite phase-separated structure in the sample by annealing for a short time at a temperature well into the two-phase region. The sample is then quenched down to a lower temperature. The two-phased structure generated would start to melt away (with a resultant decrease in scattered intensity) if the quenched temperature is in the miscible region but will continue to grow (giving an increase in scattered intensity) if the quenched temperature was within the phase-separated region. This method is particularly suitable for systems in which the temperature difference between the blend T_g and the phase boundary is small.⁷

A representative example of the procedure involved is shown in Figure 7. A STVPh[50]-PHMA with a 70:30 blend composition was first annealed at 180 °C (a temperature within the two-phase region) for a period of 20 min. The sample was then quenched back to a series of temperatures, and the scattering intensity was measured isothermally as a function of time. Thus at temperatures above 145 °C, the intensity of scattering continues to grow, implying that the system is still within the two-phase region. At 140 °C a decrease in scattered intensity is observed, indicating that at this temperature the system

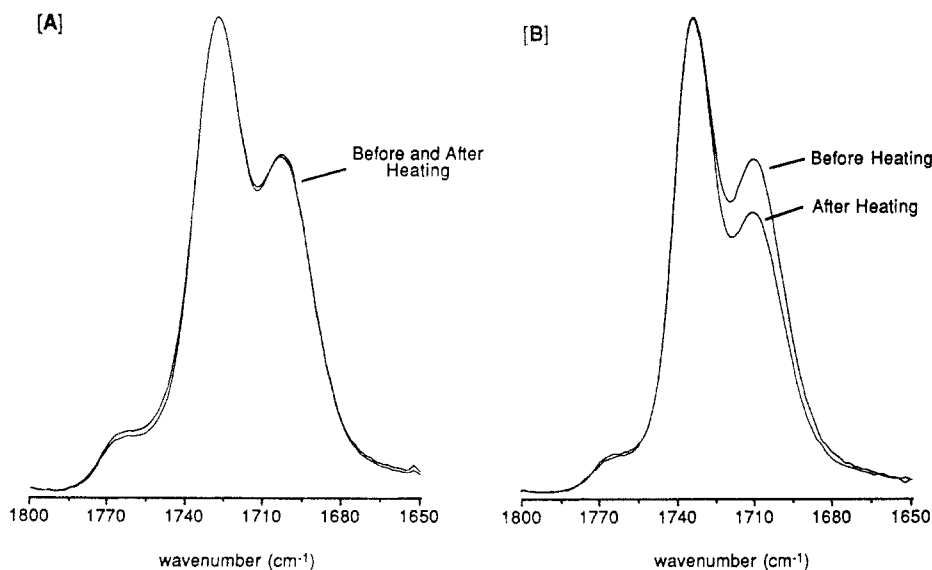


Figure 6. Scale-expanded infrared spectra of the carbonyl stretching region for [A] the STVPh[50]-PBMA and [B] the STVPh[50]-PHMA blend at a 80:20 blend composition before and after heating to 200 °C.

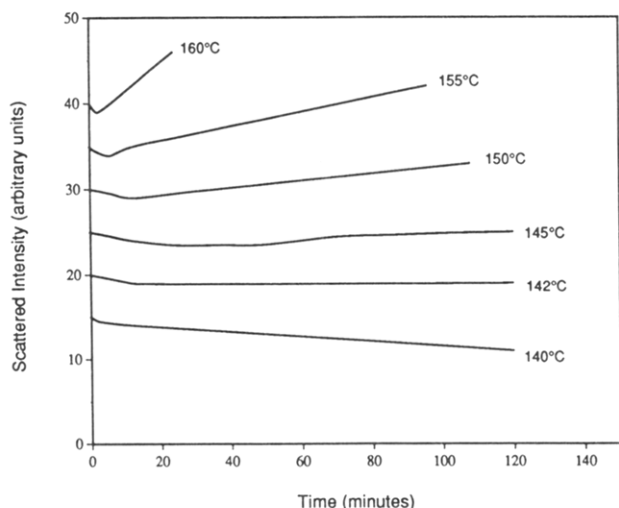


Figure 7. Reverse quench experiment to determine the phase separation temperature for STVPh[50]-PHMA 70:30 blend. The molecular weight of the PHMA used was 55 000.

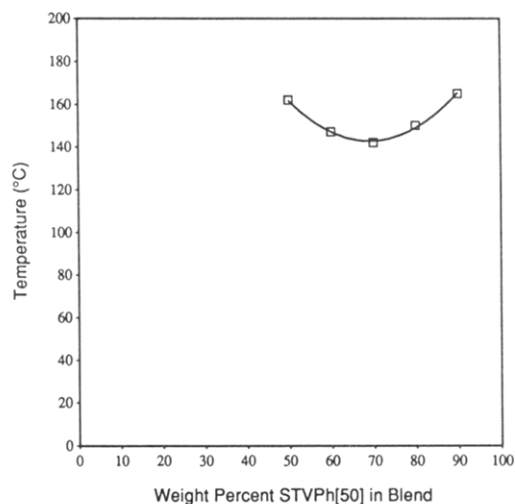


Figure 8. Phase diagrams for the STVPh[50]-PHMA blend. The solid line is arbitrarily drawn through the phase separation temperatures to aid visual observation.

is miscible. The scattering at 142 °C is almost constant, and this temperature is therefore taken as the boundary between the miscible and two-phased regions. Repetition of this procedure at all compositions allows us to map the STVPh[50]-PHMA phase diagram, shown in Figure 8. Again, there are two interesting features about the phase diagram. Firstly, phase separation occurs at the same temperature range as the systems containing much lower degrees of hydrogen bonding shown in Figure 4. Secondly, the STVPh[50]-PHMA phase diagram also shows asymmetry, but with a skewness at the other composition end compared to the systems containing lower quantities of vinyl phenol.

Discussion

In most polymer blends, miscibility is considered to be dominated by a fine balance between small contributions of combinatorial entropy, free volume, and dispersive interactions to the overall free energy of mixing. Thus small changes in, for example, the molecular weights of the component polymers cause significant effects on the phase separation temperatures and composition of the critical points. In contrast, in systems that hydrogen bond there is usually a large favorable contribution to the free energy of mixing from hydrogen bonding, which permits a sizable unfavorable contribution from dispersive interactions.¹ Miscibility can then be viewed as a *balance* between these two large and dominant effects, with contributions from compressibility and combinatorial entropy playing much smaller roles.¹⁰

The influence of these two effects in determining miscibility can be demonstrated through a "miscibility map," shown in Figure 9. The map, calculated using the association model, provides information on the miscibility of a series of poly(*n*-alkyl methacrylates) with STVPh copolymers at 100 °C. The parameters utilized are given in Table 2. Self-association between the vinylphenol groups are described by the equilibrium constants K_2 and K_B , while K_A describes the interassociation between the vinylphenol and methacrylate groups.¹ The unfavorable dispersive interactions are proportional to the difference in the constituent solubility parameters using the conventional Hilderbrand form.³ (Details of the computations have already been presented in refs 1 and 11 and are not

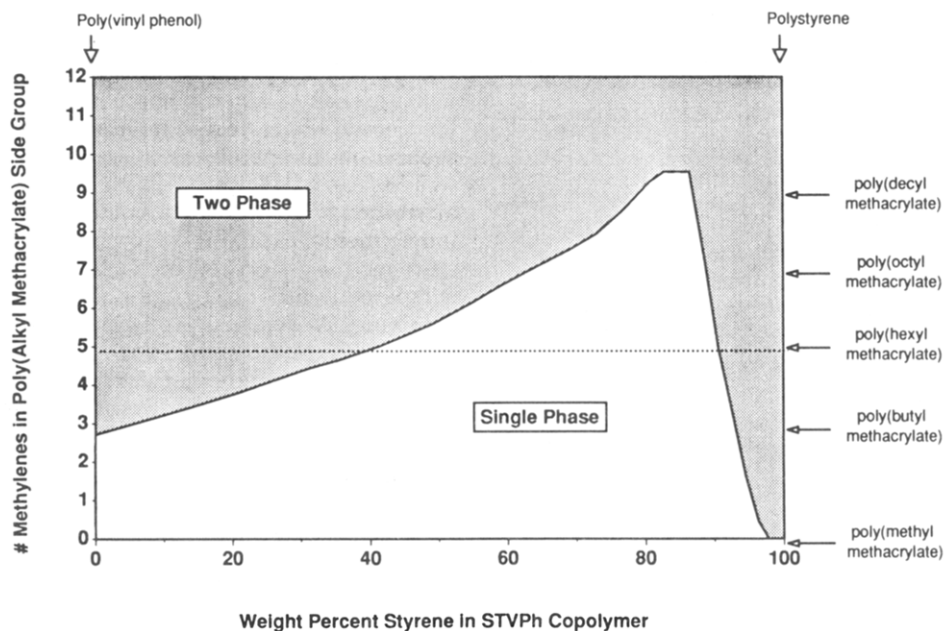


Figure 9. "Miscibility map" calculated at 100 °C for a series of poly(alkyl methacrylates) with styrene-*co*-vinylphenol.

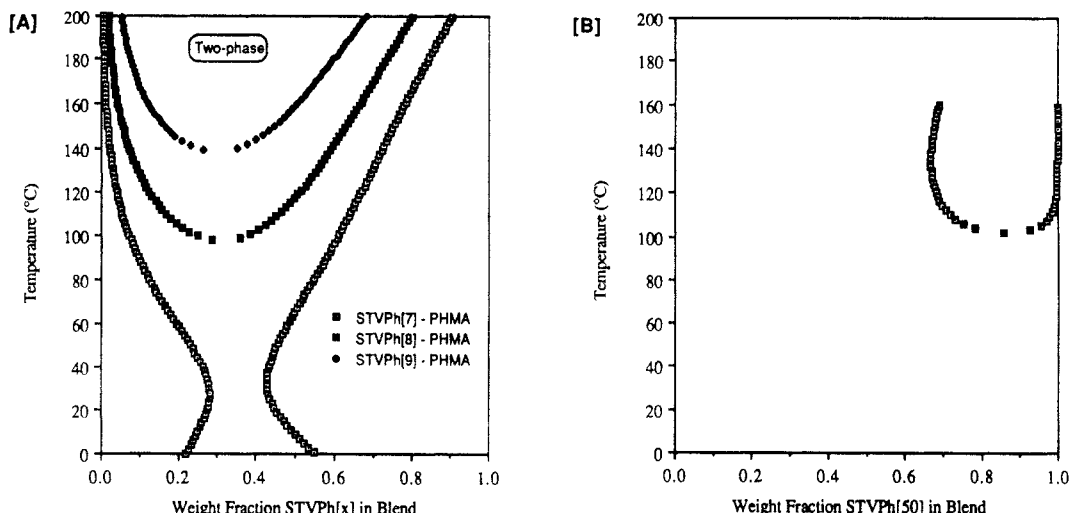


Figure 10. Theoretically predicted binodal phase diagrams for [A] blends of PHMA with STVPh copolymers containing 7, 8, and 9% VPh and [B] STVPh[50]-PHMA.

Table 2. Parameters Utilized in Theoretical Calculations^a

segments	molar volume (cm ³ /mol)	solubility parameter (cal-cm ⁻³) ^{-0.5}	equilibrium constants of hydrogen bond formation at 25 °C		
			K_2	K_B	K_A
vinylphenol	100.0	10.6	21.0	66.8	
styrene	93.9	9.5			
methyl methacrylate	84.9	9.1			37.5
methylene	16.5	8.0			

^a Enthalpy of hydrogen-bond formation: $h_2 = 5.6$, $h_B = 5.2$, $h_A = 3.75$ kcal/mol.

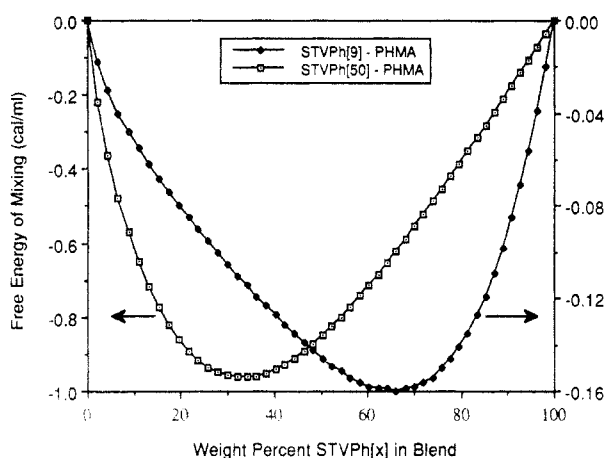


Figure 11. Free energy curves predicted by the association model at 100 °C for the blends indicated.

repeated here.) Consider, for example, the blends of PHMA with STVPh copolymers. Pure polystyrene is immiscible with PHMA, but the addition of only a small fraction of vinylphenol (~7%) causes the STVPh copolymer to be miscible with PHMA. This is a direct consequence of the favorable hydrogen-bonding interactions introduced between the two polymers. However, the introduction of the vinylphenol units also causes an increase in the unfavorable dispersive interactions (due to an increase in solubility parameter of the STVPh copolymer). At a certain copolymer composition (~50 wt % vinylphenol), this offsets the favorable hydrogen-bonding contributions resulting in immiscibility once again.

At the boundaries between the miscible-immiscible regions, the system is at the edge of miscibility. Herein lies the greatest probability of finding blends exhibiting

phase separation as a function of temperature/blend composition. Theoretically predicted phase diagrams for these blends are shown in Figure 10. Comparisons to the experimental phase diagrams of Figures 4 and 8 are very good, although the predictions err slightly toward immiscibility. Thus the association model can predict (and explain) the changes in both the temperature of phase separation and the skewness of the phase diagram with changes in copolymer composition.

The skewness of the phase diagram in these systems is not affected by the molecular weights of the polymers (as in conventional polymer blends), but rather by the balance between the self-associating and interassociating hydrogen bonds. This can clearly be seen from the free energy curves predicted by the association model (that incorporates these effects) for the PHMA blended with copolymers containing small amounts of vinylphenol groups (STVPh[9]) and those containing larger amounts of vinylphenol groups (STVPh[50]) shown in Figure 11. For the STVPh[9]-PHMA system, the free energy curve is skewed toward higher STVPh[9] blend compositions. This causes the first signs of instability (or phase separation) to occur at the other end of the composition range, giving an asymmetric phase diagram. The same holds true for the STVPh[50]-PHMA system. (This skewness is also observed by other experimental phase diagrams on similar hydrogen-bonded polymer blends.^{7,9})

A number of experimental investigations have been focused on the effects of molecular weight on the phase separation temperatures.² An increase in molecular weights causes a lowering in phase boundaries, generally attributed to the decrease in combinatorial entropy (which is detrimental to mixing). However, for hydrogen-bonded systems the effect of molecular weight is negligible compared to other contributions to the thermodynamics of mixing. As demonstrated by the observations in Figure 5, although the dynamics of the phase separation process are affected by the molecular weights, the static (equilibrium) properties (or temperatures at which separation occur) remain the same.

Acknowledgment. The authors gratefully acknowledge the financial support of the National Science Foundation, Polymers Program.

References and Notes

- (1) Coleman, M. M.; Graf, J. F.; Painter, P. C. *Specific Interactions and the Miscibility of Polymer Blends*; Technomic Publishing, Inc.: Lancaster, PA, 1991.

- (2) Painter, P. C.; Graf, J. F.; Coleman, M. M. *J. Chem. Phys.* **1990**, *92*, 6166.
- (3) Coleman, M. M.; Serman, C. J.; Bhagwagar, D. E.; Painter, P. C. *Polymer* **1990**, *31*, 1187.
- (4) (a) Malcom, G. N.; Rowlinson, J. S. *Trans. Faraday Soc.* **1957**, *53*, 921. (b) Nord, F. F.; Bier, M.; Timasheff, N. *J. Am. Chem. Soc.* **1951**, *73*, 289.
- (5) (a) Pearce, E. M.; Kwei, T. K.; Min, B. Y. *J. Macromol. Sci.-Chem.* **1984**, *A21* (8 and 9), 1181. (b) Ahn, T. O.; Eum, H. S.; Jeong, H. M.; Park, J. Y. *Polym. Bull.* **1993**, *30* (4) 461. (c) Crowie, J. M. G.; Reilly, A. A. N. *J. Appl. Polym. Sci.* **1993**, *47*, 1155.
- (6) Akiyama, S.; Ishikawa, K.; Fujiishi, H. *Polymer* **1991**, *32*, 1673.
- (7) He, M.; Liu, Y.; Feng, Y.; Jiang, M.; Han, C. C. *Macromolecules* **1991**, *24*, 464.
- (8) Xu, Y.; Graf, J. F.; Painter, P. C.; Coleman, M. M. *Polymer* **1991**, *32*, 3103.
- (9) Serman, C. J.; Painter, P. C.; Coleman, M. M. *Polymer* **1991**, *32*, 1049.
- (10) Graf, J. F.; Painter, P. C.; Coleman, M. M. *J. Phys. Chem.* **1991**, *95*, 710.
- (11) Xu, Y.; Painter, P. C.; Coleman, M. M. *Makromol. Chem. Makromol. Symp.* **1991**, *51*, 61.
- (12) (a) Nishi, T.; Kwei, T. K. *Polymer* **1975**, *16*, 285. (b) Kwak, K. D.; Okada, M.; Nose, T. *Polymer* **1991**, *32*, 864. (c) Horiuchi, H.; Irie, S.; Nose, T. *Polymer* **1991**, *32*, 1970.